

FOURTH EUROPEAN ROTORCRAFT AND POWERED LIFT AIRCRAFT FORUM

Paper No. 5

OPTIMIZATION OF JET DISTRIBUTION ALONG THE BLADE  
FOR VTOL JET PROPELLED ROTOR

V. FIORINI  
Scuola di Ingegneria Aerospaziale  
Roma

E. SANTORO  
Università di Salerno  
Salerno

September 13 + 15, 1978

STRESA - Italy

Associazione Italiana di Aeronautica ed Astronautica  
Associazione Industrie Aerospaziali



## 1. - Introduction

Considerable advances have taken place in aircraft wing design but, until now, no comparable progress has been made in the field of aircraft propeller.

Recently the solution of jet propeller rotor that might offer attractive simplification from design point of view owing to fluidodynamic transmission of power has been proposed for S/VTOL applications. An aircraft propeller generates thrust by imparting a change of momentum to the air passing through the disc and this thrust has to vary according to the operating conditions of the aircraft. Thrust requirements within the flight envelope are much broader for a VTOL aircraft than for a conventional one. It can be assumed that in the vertical flight/hovering conditions the propeller thrust is about 10 times greater than in cruise. The corresponding ratio of engine power is of the order of 3 or more. With the exception of tilting rotors with mechanically variable blades the same propeller is used in hovering for vertical thrust generation and in cruise as a source of propelling thrust.

As a result of this double role the conflicting blade design requirements such as blade diameter, twist and RPM for the two propeller regimes are well known. Going from minimum to maximum blade pitch the thrust can be more than doubled for a rotor. Another factor of two can be obtained by increasing the rotor RPM of 40% (i.e. with corresponding tip speed variation from 180 m/s to 250 m/s) at maximum pitch. It still remains another factor of about two to be introduced to meet the hovering requirements in terms of thrust that are usually specified at 6000 ft at ISA + 10° condition. This increase of thrust can only be obtained by increasing the conventional propeller diameter which for similarity rule has to increase of about 20%. For the cruise regime this increase of diameter causes a penalty due to increased propeller drag and weight which lowers the cruise efficiency. To overcome this penalty sophisticated solutions have been proposed such as variable diameter rotors (up to 15% diameter reduction in cruise) or variable twist rotors that add mechanical complexity and weight to the system.

A jet propelled rotor with optimum distribution of the jet along the outer portion of the blade span increasing the circulation along the blade by jet flap effect, offers a substantial increase in thrust in hover with corresponding reduction of the rotor diameter in cruise. In addition the simplification offered by fluidodynamic transmission of power allows a substantial reduction in mechanical complexity with respect to the driving and interconnecting mechanism for thrust generation and thrust vector rotation when mechanical transmission of power is used.

1) JET PROP-ROTOR IN FORWARD FLIGHT

In a previous work (Re.1) the hovering condition for a jet propelled prop-rotor with optimum distribution of the efflux along the outer portion of the blade span (30%) has been given. In the present study we shall derive the corresponding optimum jet distribution along the blade for the same prop-rotor in forward flight.

Before examining the case of jet propeller rotor the basic equations for a conventional prop-rotor following blade element theory are given. With reference to fig. 0 and by means of well known equilibrium conditions along the thrust axis and drag axis the thrust coefficient and the induced torque coefficient are given in adimensional notation by :

$$\begin{aligned}
 (1) \quad C_T &= \sigma \int_{.2}^{.97} (\lambda^2 + x^2) C_L \cos(\phi + \alpha_i) (1 + \epsilon t_g(\phi + \alpha_i)) dx = \\
 &= C_{T_1} \int_{.2}^{.97} + C_{T_2} \int_{.2}^{.97} \\
 C_{Q_i} &= \sigma \int_{.2}^{.97} x (\lambda^2 + x^2) C_L \cos(\phi + \alpha_i) (\epsilon + t_g(\phi + \alpha_i)) dx = \\
 &= C_{Q_{i1}} \int_{.2}^{.97} + C_{Q_{i2}} \int_{.2}^{.97}
 \end{aligned}$$

For the profile drag the corresponding torque coefficient is given by

$$(2) \quad C_{Q_o} = \sigma \int_{.2}^{.97} C_D x \cos(\phi + \alpha_i) (\lambda^2 + x^2) dx$$

From momentum considerations the following equation for the induced velocity angle with ipohthesis of neglecting its tangential component can be written (with usual approximation

$$(3) \quad \alpha_i = \frac{1}{2} \left[ \left( \frac{\lambda}{x} - \frac{\sigma a_o}{8 x^2} (\lambda^2 + x^2)^{\frac{1}{2}} \right) + \sqrt{\left( \frac{\lambda}{x} + \frac{\sigma a_o}{8 x^2} (\lambda^2 + x^2)^{\frac{1}{2}} \right)^2 + \frac{\sigma}{2 x^2} (\lambda^2 + x^2)^{\frac{1}{2}} a_o (\beta - \phi)} \right]$$

In previous equations (1) thrust and induced torque coefficients have been written as the sum of two terms in order to have separate equations for the contributions of the outer portion of the blade span (X from 0,7 to 0,97). In the following part we shall derive separate formula for thrust and induced torque contributions  $(CT_2)_J$  and  $(CQ_{i2})_J$  of the outer portion of the blade when the jet efflux of mass flow  $\dot{m}$  for unit span and jet angle  $\gamma$  is present.

In accordance with jet flap theory (Ref NASA.TN... and .A....) the jet efflux along the blade span induces a supercirculation that increases both basic lift and induced drag coefficients of the section profile considered. In the present work according to Ref. L... no increase of profile drag due to the presence of jet flap is taken into account with respect to basic drag coefficient of the profile. If a jet of mass flow  $\dot{m}$  per unit span and jet angle  $\gamma$  is present, the increase of lift coefficient  $C_L'$  is as follows :

$$(4) \quad \begin{aligned} C_D' &= C_D \\ C_L' &= a_0(\beta - \phi - \alpha_i) + 3.18\sqrt{C_J}(\beta + \gamma - \phi) \end{aligned}$$

$$\text{where } 3.18\sqrt{C_J} = \frac{K'\sqrt{C_{\mu}}}{(\lambda^2 + x^2)^{1/2}} \quad K' = 3.18\sqrt{\frac{W_J}{\rho R}}$$

For the induced velocity angle when jet flap effect is present the moment balance leads to the following new equation (by neglecting second order terms) :

$$(5) \quad \alpha_i' = \frac{1}{2} \left[ -\frac{\lambda}{x} - \frac{\sigma}{8x^2}(\lambda^2 + x^2)^{1/2} + \sqrt{\left(\frac{\lambda}{x} + \frac{\sigma}{8x^2}(\lambda^2 + x^2)^{1/2}\right)^2 + (a_0(\beta - \phi) + \frac{K'\sqrt{C_J}(\beta + \gamma - \phi)\sigma}{2x^2}(\lambda^2 + x^2)^{1/2})^2} \right]$$

that for  $C_J = 0$  gives again equation (3)

Equations (1) still apply to the jet propelled rotor case if we replace the above derived expressions of  $C_L'$  and  $\alpha_i'$  for the  $CT_2$  and  $CQ_{i2}$  terms. By so doing we write explicitly :

$$(6) \quad \begin{aligned} C_{T_{2J}} &= \int_{.2}^1 (\lambda^2 + x^2) \left( a_0(\beta + \phi - \alpha_i') + \frac{K'\sqrt{C_{\mu}}}{(\lambda^2 + x^2)^{1/2}} (\beta + \gamma - \phi) \right) (1 - \varepsilon' t_g(\phi + \alpha_i')) \cdot \\ &\quad \cdot \cos(\phi + \alpha_i') dx \\ C_{Q_{2J}} &= \int_{.2}^1 (\lambda^2 + x^2) x \left( a_0(\beta + \phi - \alpha_i') + \frac{K'\sqrt{C_{\mu}}}{(\lambda^2 + x^2)^{1/2}} (\beta + \gamma - \phi) \right) (\varepsilon' + t_g(\phi + \alpha_i')) \cdot \\ &\quad \cdot \cos(\phi + \alpha_i') dx \end{aligned}$$

The final expression for the thrust and torque ex efficient of the jet propelled rotor are :

$$(7) \quad C_T = C_{T_1} + C_{T_2J}$$

$$C_{Q_d} = C_Q = C_{Q_{i_1}} + C_{Q_{i_2J}} + C_{Q_0}$$

where the total torque coefficient derived by adding to induced torque coefficient the profile drag torque coefficient has been placed equal for dynamic equilibrium to the torque available coefficient  $C_{Q_d}$ . From Ref.1... by straight forward derivation the expression of  $C_{Q_d}$  is then:

$$(8) \quad C_{Q_d} = \sigma \int_{r_2}^1 c_{\mu} x^2 \left( \frac{K}{x} \cos(\beta + \gamma) - 1 \right) dx$$

By analogous reasoning as per Ref.1 the corresponding definition of jet propulsive efficiency can be written in forward flight for the x section :

$$(9) \quad \eta_p = \frac{2 \left( \frac{K}{x} \cos(\beta + \gamma) - 1 \right)}{\left( \frac{K}{x} \right)^2 - \left( \frac{K}{x} \right)^2 - 1}$$

Once  $K(x) = \frac{W_j}{\Omega R}$  is given, the propulsive efficiency is strongly dependent upon the blade pitch and jet efflux angle. In the present study the average value of  $\eta_p$  has been evaluated along the jet covered part of the blade span in order to write the total efficiency of the jet prop-rotor as the product of the aerodynamic efficiency of the prop-rotor times the mean propulsive efficiency

$$(10) \quad \eta_T = \eta_{pm} \frac{C_T \lambda}{C_Q}$$

## 2) OPTIMIZATION OF JET DISTRIBUTION

The distribution of jet efflux defined by jet mass flow and jet angle with zero lift axis of the blade profile was varied along the outer blade

span in order to optimize the rotor figure of merit in the hovering case per Ref.4..... By means of variational calculus taking into account the constraints given by the dynamic equilibrium of the jet propelled blades for a given rotor thrust, the optimum distribution of the jet efflux was then derived.

In order to derive the optimum distribution of the jet along the blade when the prop-rotor is in forward flight after having accomplished the transition phase (not covered by the present analysis) we have now imposed the condition of constant aerodynamic efficiency along the blade (Betg condition). Starting from the well known aerodynamic efficiency definition written for the profile at section  $x$  with usual notations a relationship between the mass flow coefficient of the jet  $C_{\mu}$  and the jet angle  $\gamma$  was obtained :

$$(11) \quad \beta + \gamma - \phi = \frac{f(x)}{\sqrt{C_{\mu}}}$$

where

$$f(x) = \left( \frac{k^2 + x^2}{k^1} \right)^{1/2} \left[ \frac{C_{R0}}{\eta_e - 1} \left( \frac{x^2 - k^2}{xk} - a_0(\beta - \phi) \right) \right]$$

Eq. 11 looks rather similar (a part from the different expression for  $f(x)$ ) to eq. 2.3 of Ref.1 derived for the hovering condition by imposing the local figure of merit of the blade to be constant along the jet flapped portion of the blade. A known relationship between  $C_{\mu}$  and  $\gamma$  is obtained since imposing the boundary condition (i.e. the  $C_{\mu}$  and  $\gamma$  at the blade section for  $x = 1$ )  $f(x)$  can be calculated along the blade span. We have than reduced the number of variable to be determined from two to one namely :  $\gamma(x)$ .

The available jet power per unit span is given by

$$\frac{\dot{m}}{2} (W_J^2 - R^2 R^2 (k^2 + x^2)) R dx$$

that with usual adimensional notation brings to express the available power coefficient as :

$$12) \quad C_P = \frac{\sigma}{2} \int_{.2}^1 C_{\mu} (k^2 - (k^2 + x^2)) dx$$

The variational problem investigated was to find the optimum distribution of  $\gamma(x)$  for the condition of minimum power coefficient  $C_p$  together with two relationship derived from equations (7) namely for the given value of CT and power equilibrium of the prop-rotor in forward flight.

The Langrange problem was then transformed into a Mayer problem introducing auxiliary variables as proposed by Miele in Ref. 4.

$$\varphi_1 = \frac{C_T}{\sigma} \quad ; \quad \varphi_2 = \frac{C_Q}{\sigma} \quad ; \quad \varphi_3 = \frac{C_P}{\sigma}$$

Differentiating both sides of eq. (7) and eq. (12) with respect to independent variable  $x$  we can write the following differential constraints :

$$\dot{\varphi}_1 + \kappa \sqrt{c_\mu} x (\beta + \gamma - \phi) = 0$$

$$\dot{\varphi}_2 + c_\mu x^2 \left( \frac{\kappa}{x} \cos(\beta + \gamma) - 1 \right) - \kappa \sqrt{c_\mu} x (\beta + \gamma - \phi) = 0$$

$$\dot{\varphi}_3 + \frac{c_\mu}{2} ( \kappa^2 - (\lambda^2 + x^2) ) = 0$$

After three Langrange multipliers are introduced and the augmented function is written in the form :

$$F = \lambda_1 \dot{\varphi}_1 + \lambda_1 \kappa \sqrt{c_\mu} x (\beta + \gamma - \phi) + \lambda_2 \dot{\varphi}_2 + \lambda_2 c_\mu x^2 \left( \frac{\kappa}{x} \cos(\beta + \gamma) - 1 \right) - \lambda_2 \kappa \sqrt{c_\mu} x (\beta + \gamma - \phi) + \lambda_3 \frac{c_\mu}{2} ( \kappa^2 - (\lambda^2 + x^2) )$$

The extremal arc is described by the Euler Langrange equations (making use of eq. 11)

$$\lambda_1 = \text{const} \quad \lambda_2 = \text{const} \quad \lambda_3 = \text{const}$$

$$\frac{\partial F}{\partial \gamma} = \lambda_2 \frac{f(x) x^2}{(\beta + \gamma - \phi)^2} \left( \frac{\kappa}{x} \cos(\beta + \gamma) - 1 \right)^2 + \lambda_3 \frac{f(x) \cdot 2}{(\beta + \gamma - \phi)^2} ( \kappa^2 - (\lambda^2 + x^2) ) - \lambda_2 \frac{f(x)}{(\beta + \gamma - \phi)^2} \kappa x \sin(\beta + \gamma) = 0$$



Therefore being the problem of isoperimetric nature the following relation-ship for  $\gamma$  holds :

$$13) \quad 2 \left( \cos(\beta + \gamma) - \frac{x}{K} \right) - \sin(\beta + \gamma)(\beta + \gamma - \phi) + \bar{\lambda} \left( \frac{K}{x} - \frac{x}{K} - \frac{\lambda^2}{xK} \right) = 0$$

We shall note that for  $\lambda = 0$  Eq. 13 becomes the same as Eq. 2.8 of Ref.1 that gives the optimum value of  $\gamma$  for the hovering condition. The constant value of  $\bar{\lambda}$  can then be derived by imposing the boundary conditions at the end of the blade for  $x = 1$

By so doing  $f(x)$  is also determined. We shall then verify that the minimum exists by means of the Legendre Clebsh condition that gives in this case :

$$\frac{\partial^2 F}{\partial \gamma^2} = 3 + c \tan(\beta + \gamma)(\beta + \gamma - \phi) \geq 0$$

### 3) NUMERICAL EXAMPLE

Calculations have been performed for a representative three blade propeller having  $\sigma = .146$  and a diameter of 2 m both for the hovering and the forward flight conditions. For the hovering phase formulae and the same procedure given per Ref.1 have been followed, while for the forward flight phase the present results have been utilized. The aerodynamic profile bidimensional data have been taken from Ref.2 and are produced in fig. 1 corresponding to ARAD series for a thickness ratio of 20% and Mach Number 0.53

#### a) HOVERING RESULTS

For compression ratios 1,8 and 2 the optimum thickness distribution of the jet exit area are given in fig. 2 and for two values of  $(\beta + \gamma)_1$  at the blade tip. Corresponding values of  $\gamma$  jet angle variation and  $\beta + \gamma$  along the blade are then quoted in fig. 3 for  $(\beta + \gamma)_2 = 21^\circ$  at the blade tip for the two compression ratio considered.

In fig. 3 and fig.4 the variations of the air mass flow per blade  $m$ , of the Figure of Merit MJ and the jet propulsive efficiency  $\eta_p$  are shown versus  $(\beta + \gamma)_1$  blade tip angle.

Results of the numerical example are then summarized in fig. 5

where the thrust coefficient  $C_T$  the Figure of Merit  $M_J$  of the Rotor and blade mass flow  $\dot{m}$  are illustrated as a function of the blade angle  $\beta$  at .7 Radius ( $\rho = 1,8$ ). Three values of jet efflux angle at blade tip were considered. From the results of Fig. 5 it can be seen that within the range of pitch  $\beta$  of the blade considered it is possible to double the  $C_T$  of the conventional rotor (without jet). By lowering the jet flap angle from  $15^\circ$  to  $25^\circ$  the corresponding increase of  $C_T$  is of the order of 30%. The corresponding variation of the necessary air mass flow is below 40% and for the maximum pitch considered is still below 1.6 Kg/sec per blade. The figure of Merit of the Rotor varies between .77 and .62 in the range of blade pitch considered and reaches the maximum values for the lowest value of  $\gamma_2$  as expected.

#### FORWARD FLIGHT

From the discussion of results in the hovering condition it appears that in order to fully take advantage of the jet induced circulation a variation of the jet efflux area associated with corresponding jet efflux angle variation is desirable.

If the same prop-rotor is to be used in forward flight the mechanism of variation of the jet efflux area and jet angle becomes necessary. This consideration stems from the examination of fig. 6 and Fig. 7 where the optimum distribution of the jet mass flow and corresponding jet efflux angle  $\gamma$  are given along the blade span for different advance ratios  $\lambda$  as a parameter.

The mechanism of variation proposed by Dorand utilizing a blade pneumatic trailing edge could be envisaged also for this case, but the details of this solution are beyond the scope of the present note.

In fig.8 the results of the calculation carried out by means of a computer program are given for the forward flight condition within a range of  $\lambda$  between .4 and .8.

The transition phase and the forward flight at low values of  $\lambda$  were not investigated in this phase.

It must be pointed out that the lowering of the propulsive efficiency of the jet with the increase of  $\lambda$  is the main limiting factor for the proposed jet propelled rotor solution in forward flight.

The global efficiency is therefore below the corresponding figure of the conventional rotor since the increase of the aerodynamic efficiency of the prop-rotor due to supercirculation effects does not compensate for the reduction of the mean propulsive efficiency  $\eta_{p_m}$  of the jet in the range of jet pressure ratios and rotor speeds considered.

## CONCLUSIONS

The results of theoretical calculations for a jet propelled prop rotor with ARA "D" profiles show a considerable improvement of the global Figure of Merit  $M_j = \eta_p M$  with respect to previous calculations (Ref.1). A comparison of the present results with the corresponding Figure of Merit of a conventional rotor must also take into account the efficiency of the power turbine and mechanical transmission to drive the prop rotor since the gas power supplied by the gas generator can be utilized to drive directly the jet propelled rotor or to drive the power turbine and the transmission of a conventional prop rotor. The aerodynamic figure of Merit  $M$  of the conventional rotor should then be lowered by a factor of .86 (adiabatic efficiency of the turbine .89 times the mechanical efficiency of the transmission .97). Considering the improvement of  $M$  due to jet flap effect for the jet propelled rotor the advantages in using the optimum jet distribution are twofold since the Figure of Merit  $M_j$  can be assumed greater than for the conventional rotor of about 10% and the rotor diameter smaller of about 20%.

As far as the forward flight regimes are concerned, the results of the calculations carried out for the jet prop rotor show a substantial reduction of the jet propulsive efficiency with the advance ratio, that lowers the global efficiency  $\eta_T = \eta_{pm} \eta_e$  to values of about 30 + 40% below corresponding figures of the conventional rotor (obtained as above  $\eta_T = \eta_e \cdot .86$ ). However the comparison should be made taking also into account all the advantages of the jet propelled rotor system with respect to the mechanical transmission of power such as weight reduction and greater simplicity but such an analysis is beyond the aim of the present note. (Ref. 5)

For the moment it appears that the solution proposed in the present note could be most attractive for stowed or foldable rotor applications where the prop rotor is mainly used for the hovering and transition phase.

BIBLIOGRAPHY

- 1 - V. Fiorini - Sulla condizione di volo stazionario dell'elica rotore a getto distribuito. 3° Congresso Nazionale AIDAA Torino 1975 .
- 2 - A.J. Bocci - A New Series of Aerofoil Sections suitable for aircraft Propeller. Aeronautical Journal - February 1977
- 3 - J.B. Nichols - The pressure jet helicopter propulsion system. Aeronautical Journal - Sept. 1972
- 4 - G. Leitman - Optimization Techniques - Academic Press 1962
- 5 - R. Hafner - The case for the convertible Rotor. Aeronautical Journal 1971

SYMBOLS LIST

- $a_0$  slope of the lift curve
- $b$  blade number
- $c_j$  jet coefficient =
- $c_{\mu}$  jet mass coefficient
- $c_a$  torque coefficient =
- $C_T$  thrust coefficient =
- $C_L$  lift coefficient
- $C_R$  drag coefficient
- $c$  blade chord
- $C_{ad}$  torque available coefficient
- $\dot{m}$  jet mass flow per unit lenght
- $R$  tip blade radius
- $r$  blade radius
- $W_j$  jet efflux speed
- $\delta$  thickness of the efflux section
- $K = \frac{W_j}{\Omega R}$  = speed ratio
- $M_j$  = rotor figure of merit (hovering)
- $T$  = Rotor thrust
- $Q$  = Rotor Torque

$$c_{\mu} = \frac{\dot{m}}{\frac{1}{2} \rho \Omega R c}$$

$$Q = \frac{1}{2} \pi \Omega^2 R^5$$

$$T = \frac{1}{2} \pi \Omega^2 R^4$$

$$M_j = \eta_{pm} M = \eta_{pm} \cdot 707 \frac{C_T^{3/2}}{C_{Qd}}$$

Greek listing

- $\alpha$  angle of incidence
- $\beta$  blade angle
- $\gamma$  jet efflux angle
- $\epsilon$  =  $1/E$  inverse of the Efficiency
- $\rho$  = air density
- $\omega$  = angular velocity
- $\lambda$  = advance ratio
- $\lambda_i$  = Lagrange coefficient ( $i = 1, 2, 3$ )
- $\sigma$  = rotor solidity
- $\eta_p$  = propulsive efficiency
- $\eta_e$  = aerodynamic efficiency
- $\eta_T$  = global efficiency

SUFFIX

- $i$  induced values
- $o$  parasite drag
- $J$  jet values

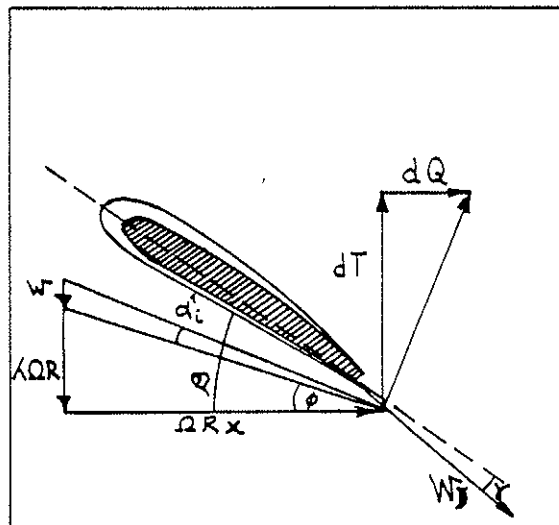


Fig. 0

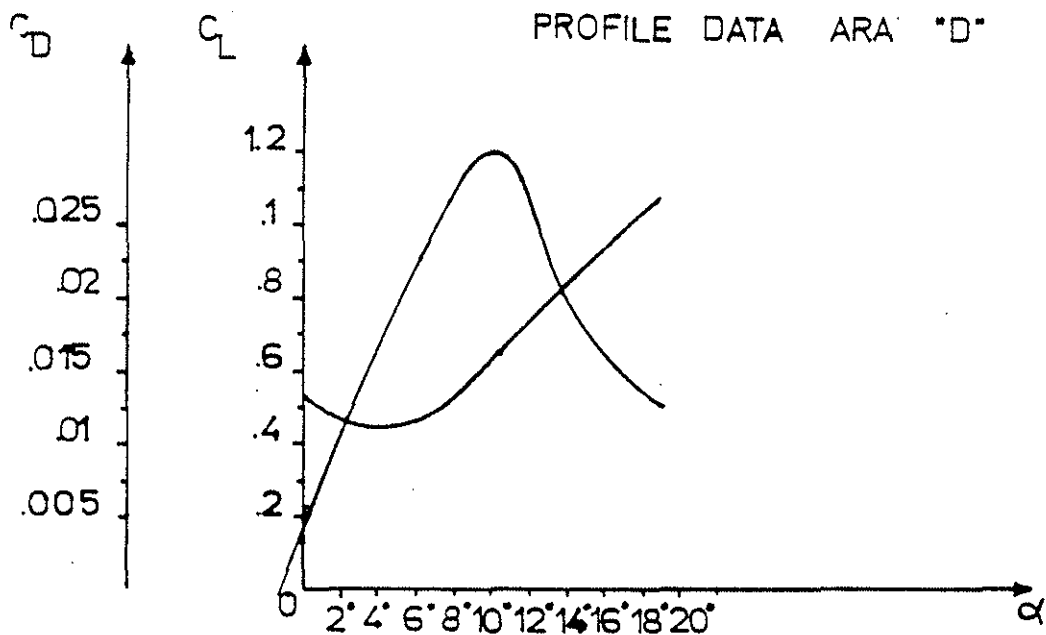


Fig.1 - Section profile aerodynamic data ARA "D" series  
( from Ref. 2) Mach Number 0.53

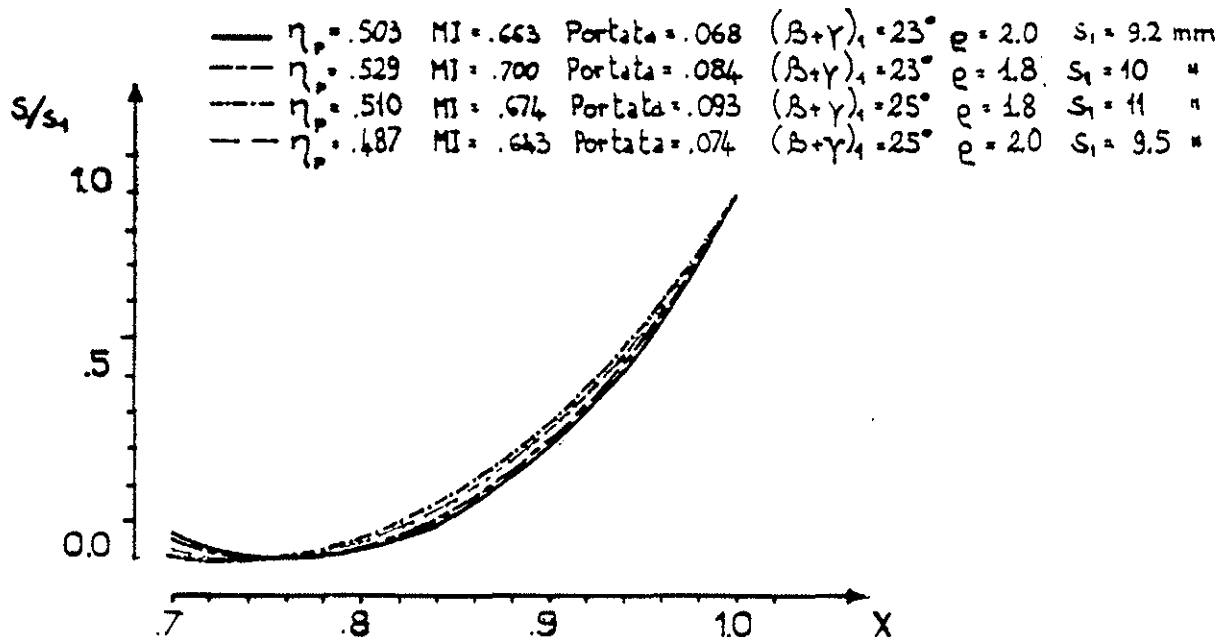


Fig. 2 - Adimensional Jet efflux area thickness  $V/S$  adimensional radius  
for different pressure ratios and  $(\beta + \gamma)_1$   
(  $\Omega R = 180$  m/s  $\sigma = .146$ ) in Hovering

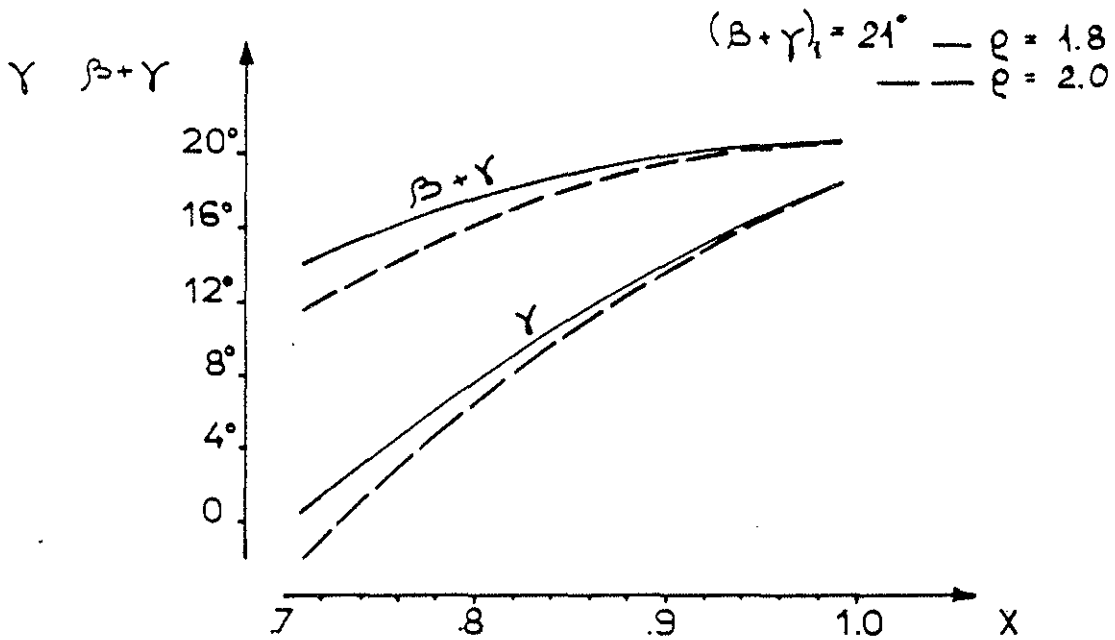


Fig. 3 - Blade pitch  $\beta$  and jet efflux angles  $\gamma$   $\forall$  dimensional radius ( $\rho = 1.8, \rho = 2, \sigma = .146, \mu R = 180^\circ$ ) in Hovering for  $(\beta + \gamma)_i = 21^\circ$

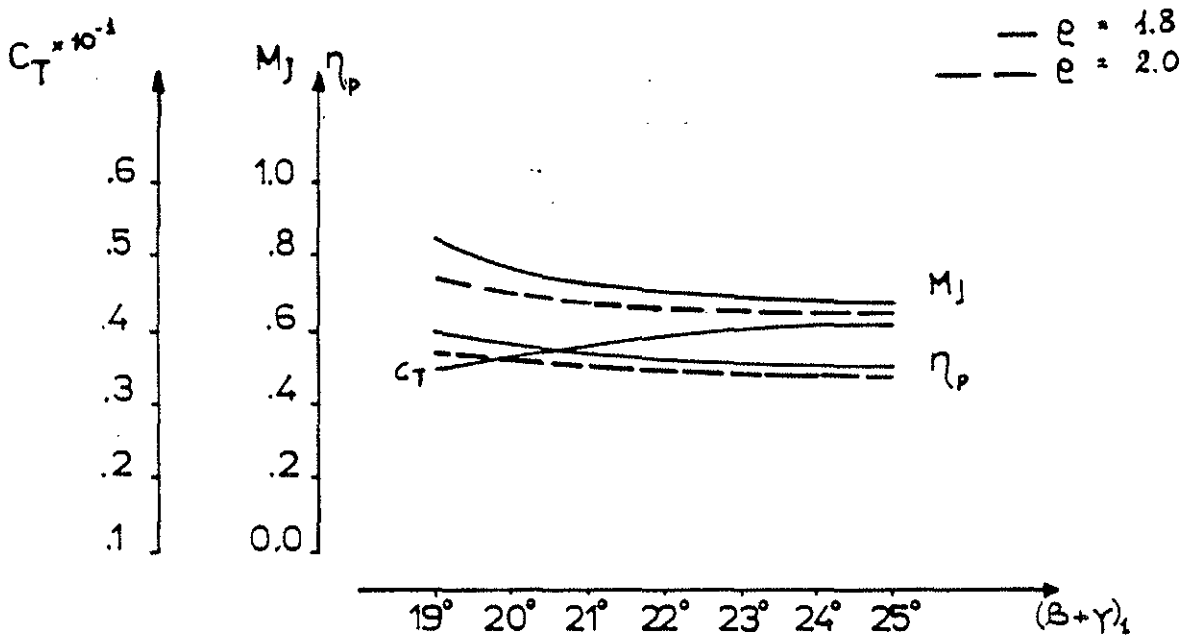


Fig. 4 - Hovering prop rotor characteristics, Figure of Merit and propulsive efficiency

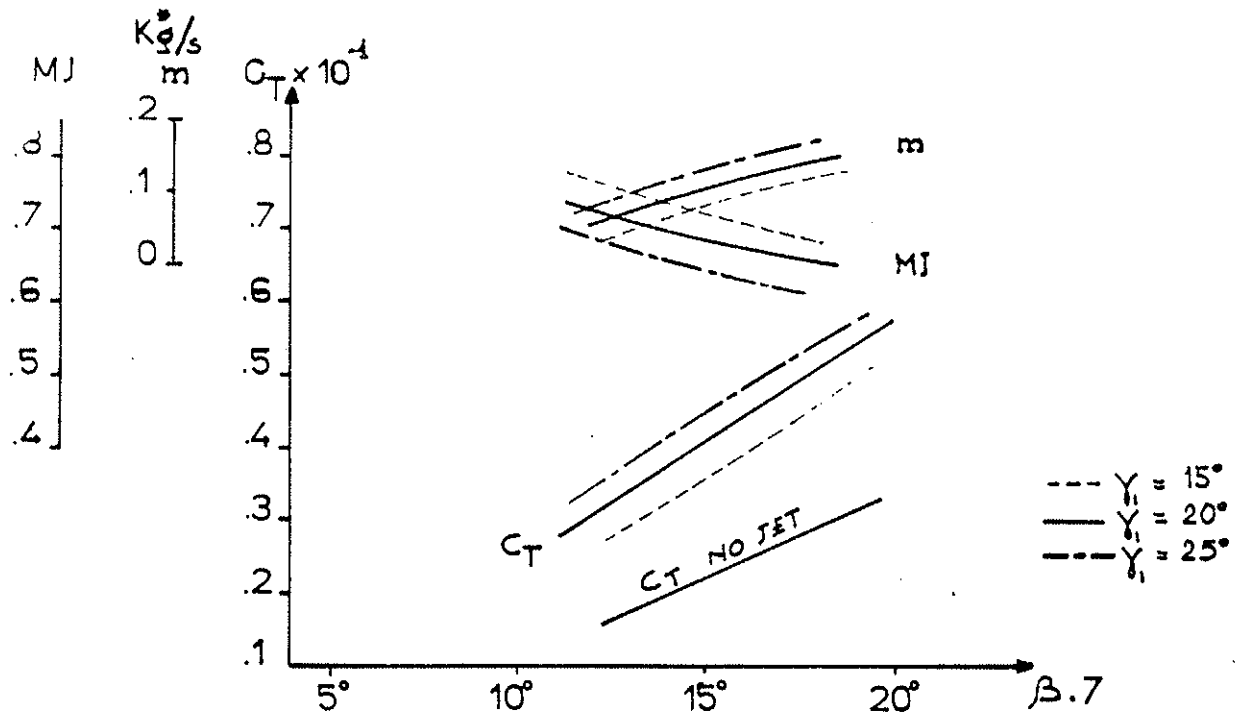


Fig. 5 - Hovering jet prop rotor map

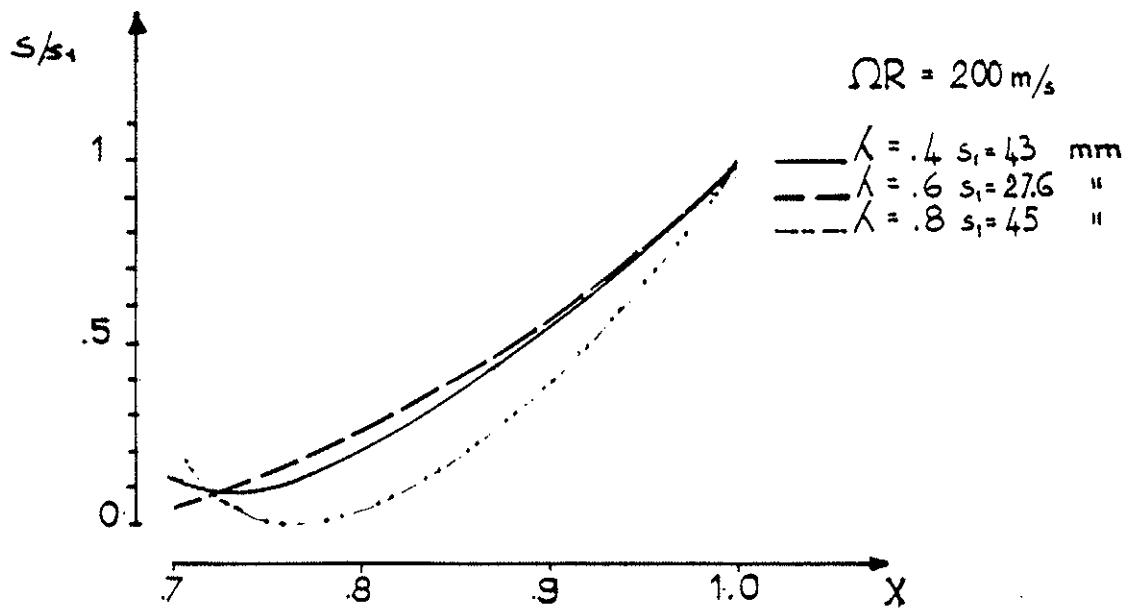


Fig. 6 - Forward Flight - Adimensional jet efflux area thickness  $V/S$  adimensional radius for different advance ratios.  $\lambda$

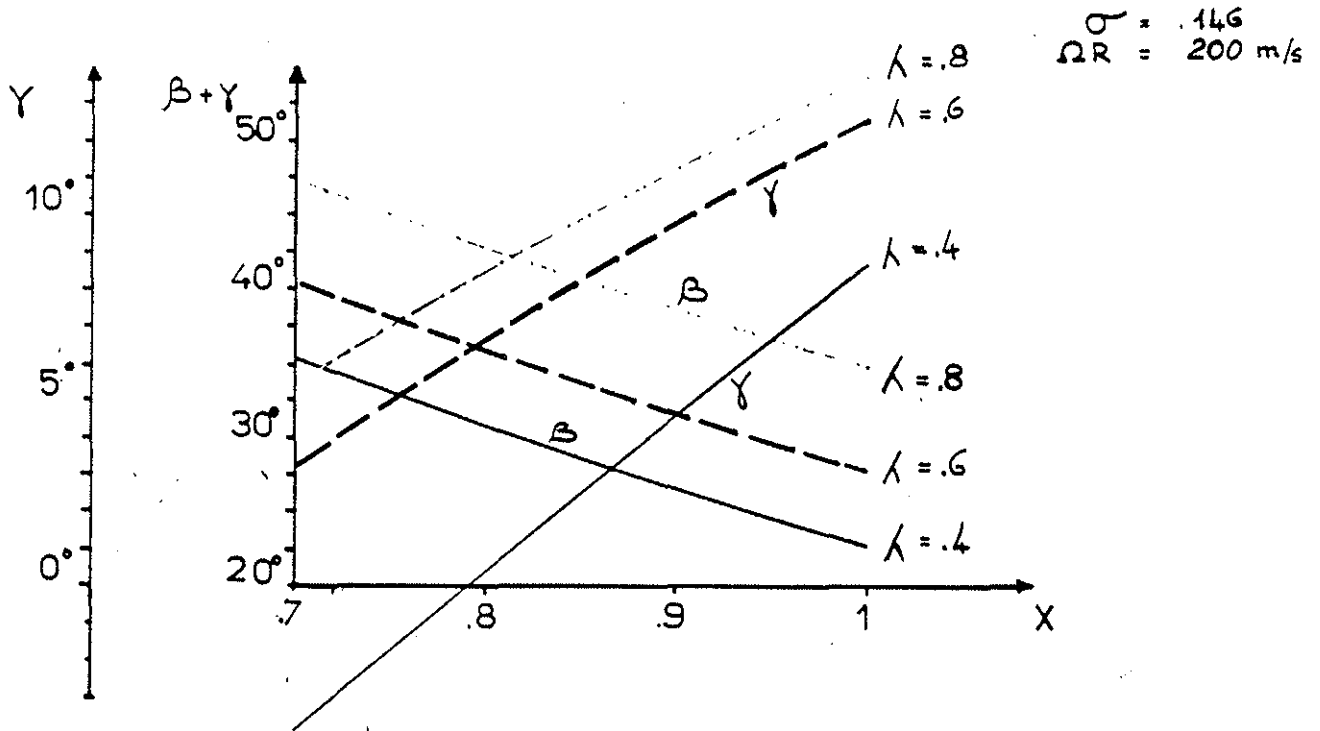


Fig. 7 - Forward flight. Blade pitch  $\beta$  and jet efflux angle  $\gamma$  v/s adimensional radius for different advance ratios  $\lambda$

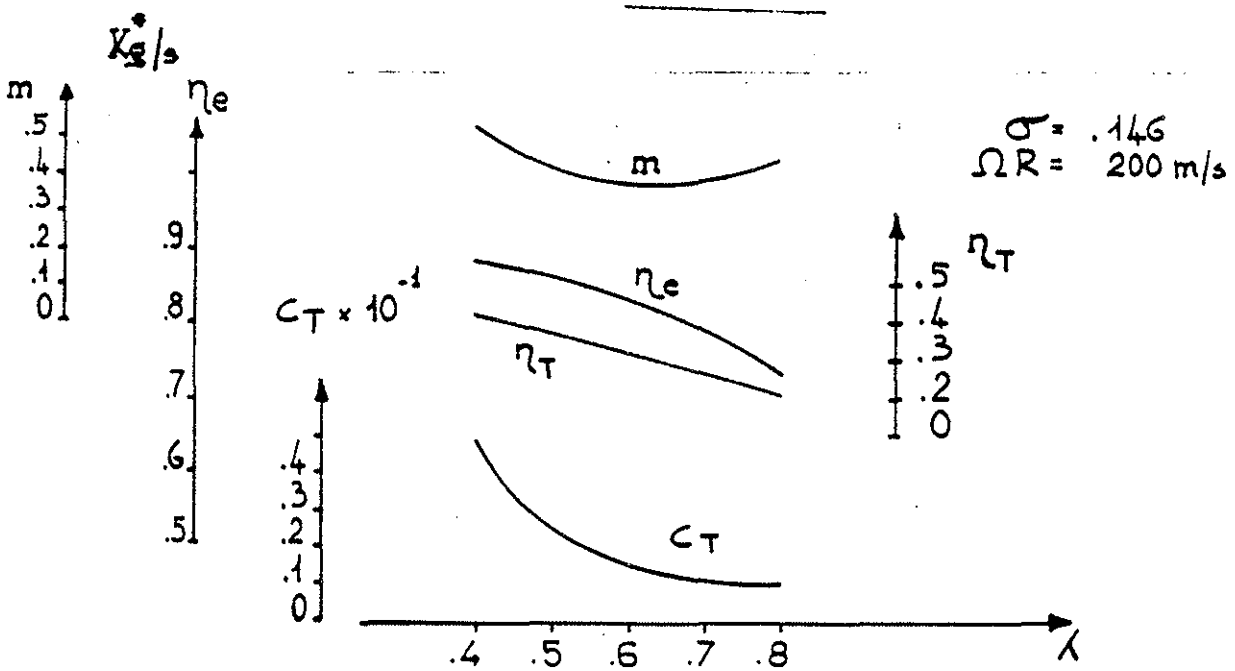


Fig. 8 - Forward flight - prop rotor characteristics